JOURNAL OF MATERIALS SCIENCE 37 (2002) 4645–4652

Manufacturing and friction welding properties of particulate reinforced 7005 Al

C. B. LIN*, I-CHIANG CHOU, C. L. MA
Department of Mechanical Engineering, Tamkang University, Tamsui, Taipei, People's Republic of China

This study has successfully incorporated Al_2O_3, SiC particulates into the 7005Al alloy matrix by using a drag-push method. The reinforced particulates are uniformly distributed in the matrix. This study also discusses the influence of aging treatment on the friction welding properties of 7005Al/10 wt%, 15 μm and 6 μm $SiC_{(p)}$ composites and 7005Al/10 wt%, 15 μm $Al_2O_{3(p)}$ composites joint system. Experimental results show that after peak aging treatment was performed, if SiC particulates were used in the strengthening phase, the heat-affected zone (HAZ) had higher density of strengthening particulate, this resulted an increase in the hardness and stress concentration at the fully plasticized zone (Zpl) of the HAZ region, but a decrease in the width of the Zpl zone and the welding strength. And the welded fracture surface morphology had a low-ductile fracture. © *2002 Kluwer Academic Publishers*

1. Introduction

Friction welding is a solid-state welding process, in which heat is generated by friction from the relative motion of the parts to be welded. The application of an axial force maintains a close contact of the parts and causes a plastic deformation of the material near the welded interface. Friction welding can be carried out at high production rates for joining similar as well as dissimilar materials. Friction welding is often used for joining particulate aluminum matrix composites (PAMCs) [1, 2], because its deformation is largely restricted to the original interface by an adiabatic shear process. The results in less input energy, and ensure that intermetallics compounds are not easily produced, thus the welding strength is increased [3]. Since less material is consumed in friction welding than in flash welding, it is more economical in application.

According to Yilbas *et al*. [4] if there are oxide films on the surface of the work piece, the friction welding strength will be lower. According to Ellis *et al*. [5] the welding strength of 2618Al/14%SiC particulate composites is about 380 N/mm^2 with friction welding. If the work piece goes through an artificial aging treatment after friction welding, the welding strength could rise to 431 N/mm^2, which is close to the 2618Al fracture stress of about 455 N/mm^2. According to Chawla *et al*. [6] the aging temperature and the aging time have a strong influence on the precipitation. As the aging temperature increases, the peak aging time for the matrix decreases rather drastically. According to Suresh *et al*. [7] a certain critical value of dislocation density can be generated even with a small reinforcement content, which serves to provide adequate heterogeneous nucleation sites for the strengthening precipitates, thereby causing accelerated aging in the composite materials. The accelerated aging of the composite matrix can affect ductility [8], ultimate tensile strength [9], and fracture resistance [10]. According to Murr *et al*. [11] the mechanical properties of 6061Al-T6 are deteriorated in the weld zone and heat affected zone, depending on the density of strengthening precipitates. According to Mahoney *et al*. [12] postweld aging produces an increase in the volume fraction of fine strengthening precipitates, which leads to an increase in strength and a decrease in ductility.

This study proposes a new melting method to make particulate reinforced aluminum alloy, and discusses the influence of aging treatment and particulate size on the welding strength of Al_2O_3, SiC particulates reinforced 7005Al matrix composites after friction welding.

2. Experimental

2.1. Materials preparation

7005Al(0.14%Zr-0.03%Ti-4.5%Zn-0.13%Cr-1.4%Mg-0.45%Mn) was used as the base material. SiC particulate of β phase and Al_2O_3 particulate of α phase whose shapes are irregular were employed as the reinforcements.

The melting equipment is shown in Fig. 1. The 7005Al was melted at 700°C, and then the molten slag was removed. The dry nitrogen was led in the melting system as a protective atmosphere. The added system and agitator were settled in a proper position in the crucible; the agitator was turned on and slowly sped up to 400 rpm. The upper and the lower impeller were then slowly sped up to 2000 rpm and

*Author to whom all correspondence should be addressed.

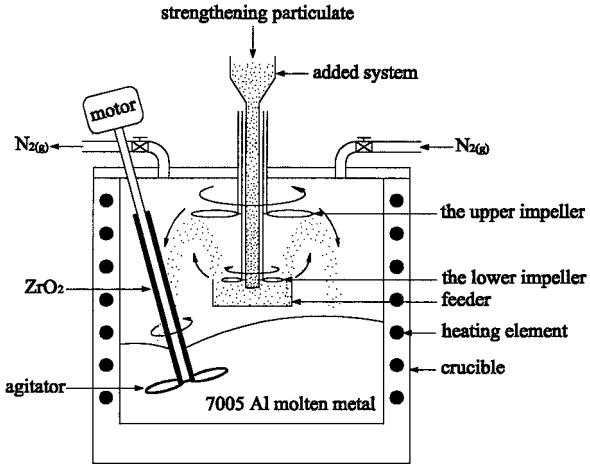

Figure 1 Schematic diagram of PAMC melting equipment system.

4000 rpm respectively. After adding certain amounts of particulate, the impellers were turned off. The agitator slowly decreased to 80 rpm, stirring was maintained for 10 min, and then it was degassed. Finally, Billets of 127 mm in diameter × 500 mm in height by using semi-continuous casting method were made. The technique described above designed for this work was employed to add 10 wt% 6 μm and 15 μm SiC particulate and 10 wt% 15 μm Al_2O_3 particulate in 7005 aluminum alloy. The abbreviation for those composites is 7005Al/6p/SiC, 7005Al/15p/SiC and 7005/15p/Al_2O_3 respectively. Then the composite billets were hot extruded at 490°C and extrusion rate of 12 l/s using a indirect extrusion machine. The billets were extruded into rods of 18 mm in diameter. To avoid the formation of inclusion within the rods, turning was employed on the surface of the billets before extruding. This would prevent a thicker oxidized layer on the surface from being drawn into the extruding plastic flow.

2.2. Friction welding

The welding workpiece pair was manufactured as shown in Fig. 2. One work piece of welding point is plane and the other is the lead angle design. Making use of this joint design can achieve a better joint strength because the tangent velocity is greater farthest from the center and smaller in the center during the process of friction welding. Thus, the materials farther from the center can produce obvious plastic flow. This plasticized zone will fill in the lead angle gap because of friction pressure. This filled plasticized zone can only hinder the following plasticized zone, which increases the chance of welding. The welding workpiece was put into a 200°C ± 3°C air furnace to anneal for two hours in order to eliminate residual stress of machining. The welding point surface Ra was 2.5 μm. Before welding, the workpiece was put into a container full of acetone, and the grease, which was on the workpiece welding planes, was removed by ultrasonic vibration. When the workpiece was spin-friction each other, the plasticization between contact planes occurred, and the plasticization began first from the periphery then to the center. The best welding strength can only be achieved with welded surfaces fully plasticized from the periphery to the center. In other words, for the best result of bonding, an ideal friction pressure with ideal friction timing is needed. Due to limitation of our spin friction-welding machine, the best friction pressure with the best friction timing of this study was 3.4 N/mm^2 and 7 secs under 730 rpm rotation speed. The finished workpiece was fixed by using the spin friction-welding machine. After fixing the two sides of the workpiece, it was friction welded; the workpiece was fixed at a rotation speed of 730 rpm, 3.4 N/mm^2 friction pressure and 7 secs friction timing. Finally a forging pressure was used for 10 secs after the friction process.

2.3. Optical microscope studies and heat treatment

All of the friction-welded workpiece sections were cut and grounded with 400-and 1200-grit carbimet papers. A final polishing was performed by using a colloidal 1 μm Al_2O_3 particulate suspension. After polishing, specimens were etched by NaOH solution ($NaOH : H_2O = 1 : 10 V_f\%$) for 30 secs in distilled water. Then the microstructure was observed through an OPTIPHOY-100 Nikon Optical Microscope (OM). After the welded flashes were machined on the friction-welded specimens, they were heat-treated using the artificial aging heat treatment. The two-step aging practice is usually used for the 7005Al to provide higher strength. A standard aging treatment for the 7005Al extrusions was solutionized at 400°C for 90 min, quenched in 22°C water, then aged artificially at 110°C for 5 hrs, followed by aging at 150°C for various time intervals, and air cooling at 22°C. The process of slow heating to the aging temperature acts as the first

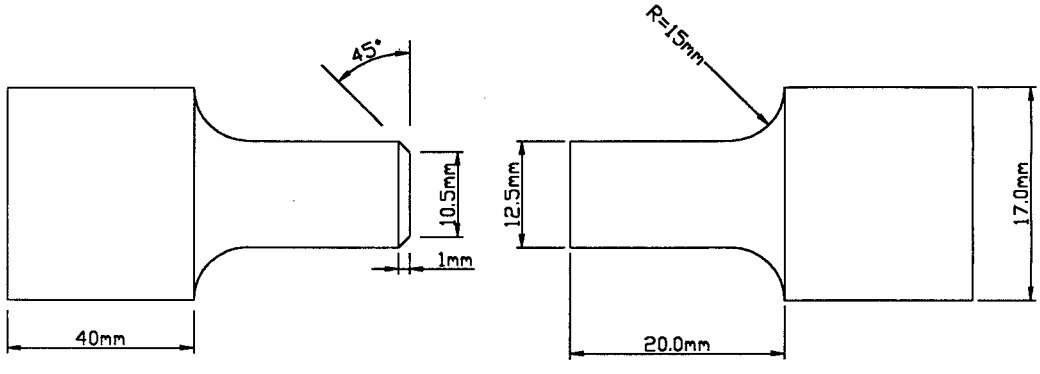

Figure 2 The size of work piece.

step in that it permits GP zones to grow to a size that does not dissolve at higher temperature [13].

2.4. Hardness and tensile test

The Akashi MVK-H11 micro-Vickers hardness tester was used to test the hardness of the welding zone. With a loading of 25 gf, a loading time of 30 secs and a loading speed of 100 μm/s. Micro-Vickers hardness profiles in the weld were measured on the cross section perpendicular to the welding direction. The hardness at each aging interval was taken to obtain the mean of six readings. The flash was machined from the welds before testing with the gauge length of the test specimen at 29 mm. All of the tensile specimens were tested at room temperature using an Instron tensile machine with a crosshead speed of 5 mm/min. The fracture stress was calculated from the load at failure divided by the original cross-section area. Three measurements were taken for each of the welding strengths to calculate their average data. A JEOL-JSM 840A-scanning electron microscopic (SEM) was used after gilding gold for 1.5 minutes to observe the tensile fracture surface morphology.

3. Results and discussion

3.1. Particulate in matrix distribution

The distribution of particulate in 7005 aluminum alloy is shown in Fig. 3, where it is evident that SiC and Al_2O_3 particulates are well distributed in the matrix, in which the uniformly degree of particulate size 15 μm is larger than 6 μm. In this paper, by using the process of molten casting, particulate 15 μm and 6 μm were uniformly added to the matrix successfully. Based upon the principle of good distribution, strengthening particulate was put in the feeder above the molten metal in the closed system, and a rotating system was installed above the feeder. While the impellers were rotating, SiC and Al_2O_3 particulates were dragged up by the lower impeller from the feeder and then pushed down by the upper impeller to be distributed on the molten metal. As soon as the particulates were pushed down on the molten surface by air pressure and their own mass, they were drawn into the molten metal vortex formed from the agitator and mixed well with the molten metal. To improve distribution, through heat convection from the molten metal, the particulate in the feeder could be continuously pre-heated to omit clustering. Producing a metal matrix composite reinforced with reinforcing material in a closed system can save nitrogen consumption, because the nitrogen gas was served only initially for purging the air outward from the system, and not consumed continuously. Compared with the conventional vortex process we can decrease the production cost of the composite can be decrease in order to increase its commercial value.

3.2. The microstructure of the particulate in the heat affected zone

According to Midling *et al*. [14] the heat affected zone (HAZ) after spin-friction welding is divided into three zones: (1) The fully plasticized region (Zpl), where the material is able to accommodate the plastic strain by dynamic recovery (or recrystallization) of the microstructure; (2) The partly deformed region (Zpd), where the degree of plastic deformation is accommodated by an increase in the dislocation density of the matrix grains. In this region the temperature is sufficiently high to facilitate dissolution of the base metal hardening precipitates; (3) The undeformed region (Zud), characterized by partial reversion of the base metal precipitates.

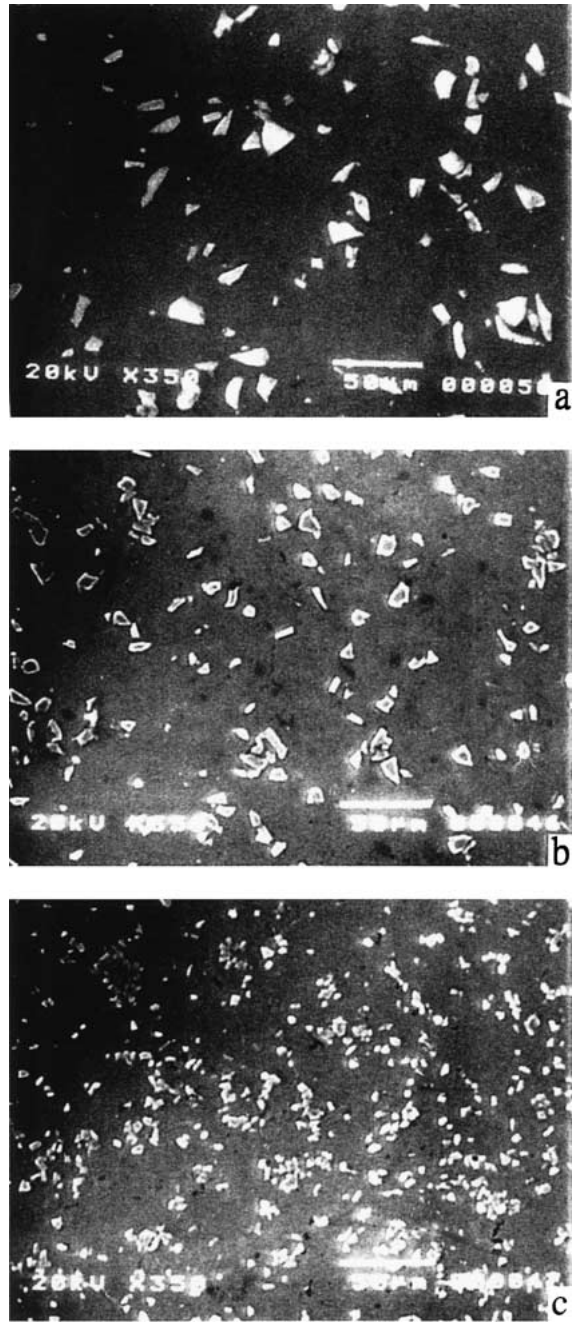

Figure 3 Microstructure of (a) 7005Al/15p/Al_2O_3 (b) 7005Al/15p/SiC (c) 7005Al/6p/ SiC composites.

In Fig. 4a, the heat-affected zone near the axial centerline after 7005Al friction welding is shown. There was an obvious plastic field in the Zpd zone during welding resulting in realignment or reorientation of the bands. The reason was that in the process of friction welding, the welding planes rotated mutually, which produced friction heat and shear stress. There was a material in the Zpd zone, which went into the Zpl zone

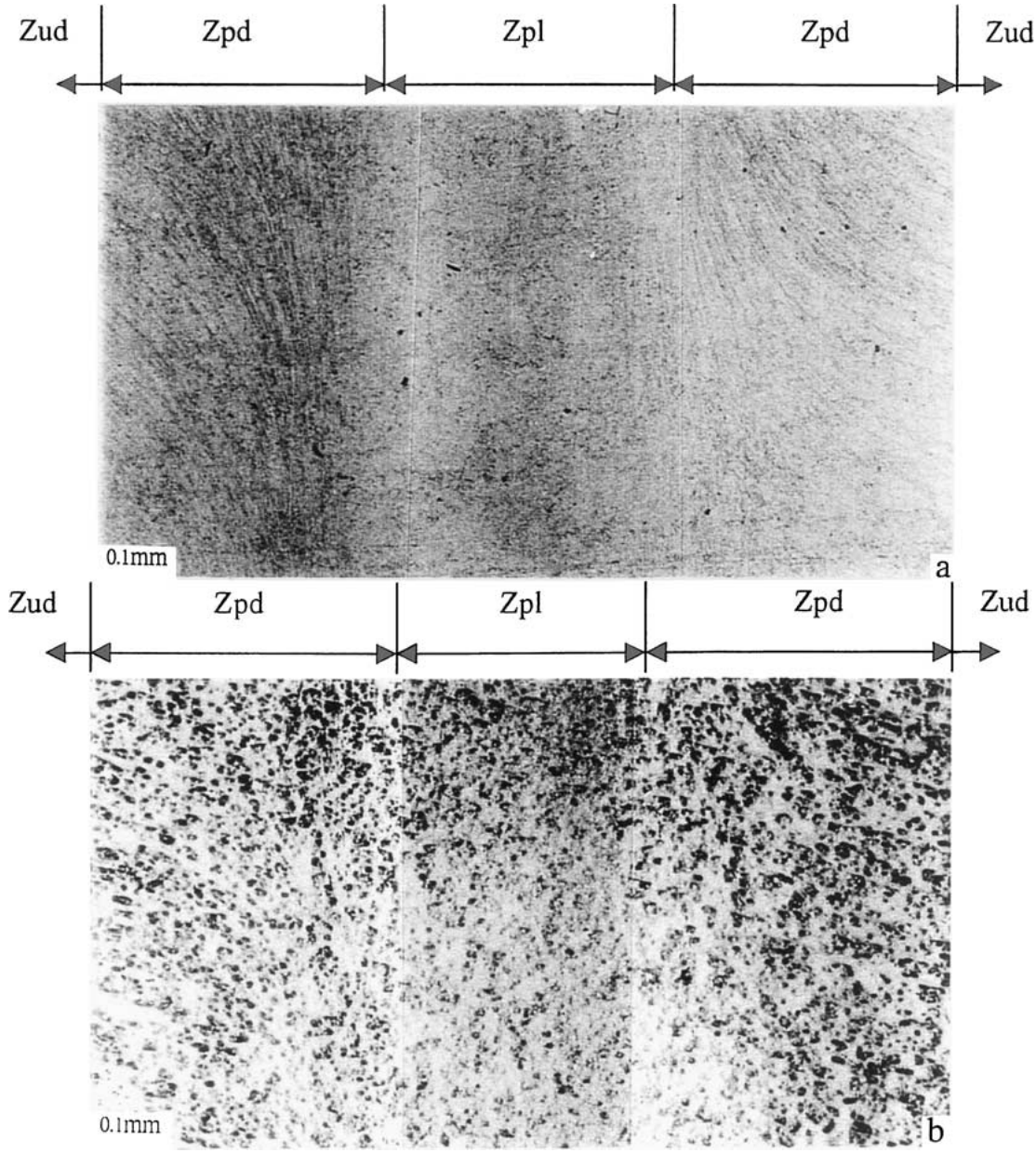

Figure 4 Microstructure of (a) 7005Al (b) 7005Al/15p/Al_2O_3 (c) 7005Al//15p/SiC (d) 7005Al//6p/SiC in the heat affected zone. (*Continued.*)

by plastic flow field direction. Friction heating and plastic flow during friction welding created a fine recrystallization grain structure around the weld center and a recovered grain structure in the thermomechanically affected zone [14].

Fig. 4b shows is the 7005Al/15p/Al_2O_3 particulate composites in the heat-affected zone. The plastic flow was less obvious in the Zpd zone than in 7005Al because the Al_2O_3 particulates could effectively prevent the plastic flow. Fig. 4c shows is the microstructure of 7005Al/15p/SiC particulate composites in the heat-affected zone. SiC particulates were distributed evenly in the Zpl zone, which was different from the orientation of Al_2O_3 particulates in the Zud of zone. There was an even more obvious plastic field in the Zpd zone than in the 7005Al/15p/Al_2O_3. This was because when spinning was employed, the softer matrix was ploughed by the harder particulate, and most of the friction heat was produced by friction of the strengthening particulate and then transferred to the matrix. Frictional heat formed per strengthening particulate $q = \tau v = \mu v H_v$, (τ: shear per particulate, v: spin velocity, μ: the coefficient of friction at plastic contact, H_v: Average Vicker's hardness). (μ, H_v) for SiC and Al_2O_3 particulate are (0.5, 3100) and (0.5, 2000). Although the coefficient of friction was changing continuously during the welding cycle, it was convenient, for simple reasons, to hold the coefficient of friction constant [15]. Thus, under an equal spinning velocity and friction pressure 7005Al/SiC composite was larger and was helpful in producing greater plastic flow in the matrix.

Fig. 4d shows are the microstructure of 7005Al/6p/SiC particulate composites in the heat-affected zone. There was an obvious plastic field in the Zpd zone because the 6 μm SiC particulates could move more easily than the 15 μm SiC and Al_2O_3 particulates in the plastic flow. Integrating Fig. 4a–d, the width of Zpl, in the 7005Al was wider (0.40 mm) than the composites, and the 7005Al/6p/SiC particulate composite (0.28 mm) was the smallest. The reason was that the particulate

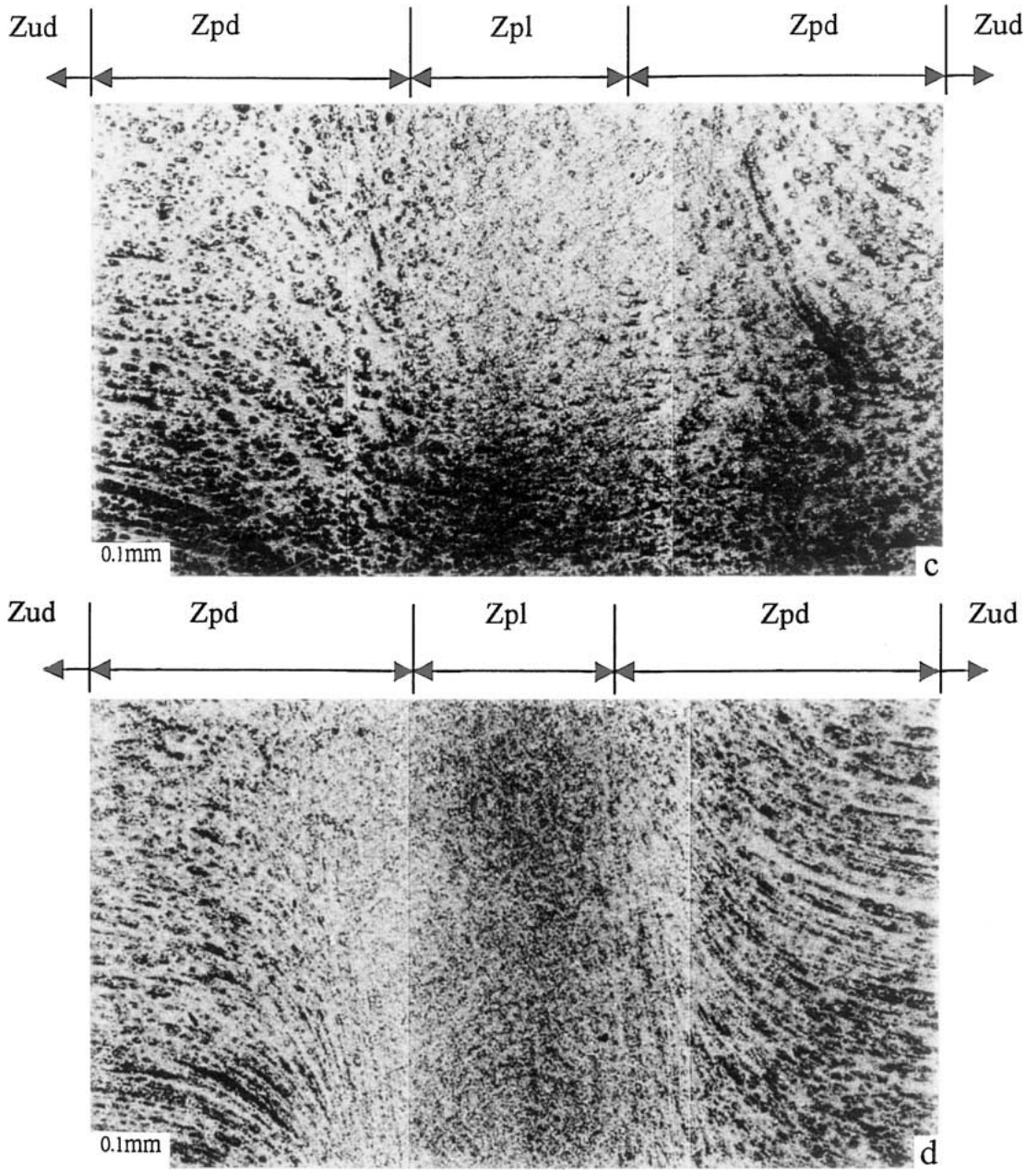

Figure 4 (*Continued*).

could restrict the plastic flow. Also, plasticization was formed because the friction heat of the composites was greater than the 7005Al base material, and the 7005Al/$SiC_{(p)}$ composites in particular produced a larger amount of friction heat than the 7005Al/$Al_2O_{3(p)}$ composite. When a forging pressure was used, the plastic field of Zpd was constricted such that its width was declined. By adding the 6 μm SiC particulate, the smallest width was obtained. As shown in Fig. 5a the Al_2O_3 particulate are distributed evenly in the matrix resulting from the extensive intermixing experience during friction welding in the Zpl zone, this is different from the orientation of Al_2O_3 particulates in the Zud zone as show in Fig. 5b. Examination of the matrix at magnification using the OM revealed that most of the Al_2O_3 particulates were clustered in a band parallel to the extrusion direction some areas contained an Al_2O_3-rich, while adjacent areas showed nearly depleted bands. The reason that Al_2O_3 particulates in the Zud zone moved to the Zpl was that the plastic flow and shear stress under friction welding created Al_2O_3 particulate composites again, which was helpful for even mixing. According to Brechet [16], during hot working at high strain, the metal matrix composites will be crashed. Thus, if applied a greater friction pressure and spinning velocity were applied a larger plastic deformation could be produced. This would cause SiC particulates close to the band line to break into a smaller size as shown in Fig. 5c, and to move into the Zpd by plastic flow to give a finer dispersion.

3.3. The hardness of the heat affected zone

According to Lin *et al.* [17] the hardness of the heat-affected zone is divided into three zones: The first zone is the Zud zone, where hardness is that of the base material. The second zone is the Zpl zone, and the third zone is the Zpd, where hardness is the transformation

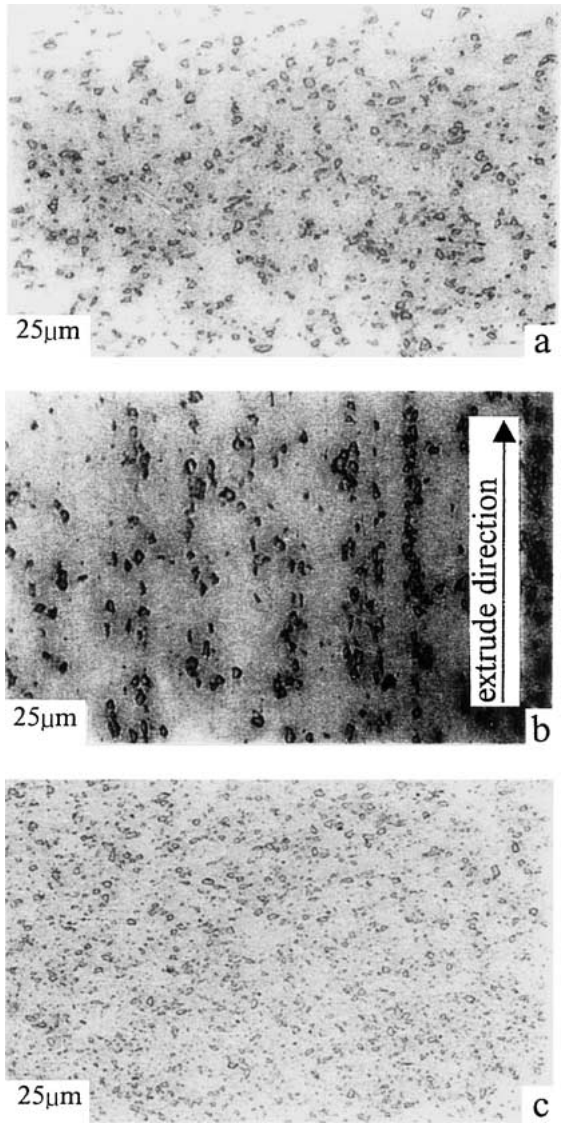

Figure 5 Microstructure of 7005Al/15p/SiC composites in (a) the Zpl zone (b) the Zud zone and (c) 7005Al//6p/SiC composites in the Zpl zone.

zone, wherein the hardness of the Zpl zone is the largest, and the hardness of the composites in the Zpl zone is greater than the Zpd and the Zud.

Comparing the peak hardness of 7005Al, 7005Al/15P/Al_2O_3 7005Al/15P/SiC at the Zpl, Zpd and Zud zones, the peak hardness of the Zpl zone was the largest and peak hardness of the Zpd zone was the smallest at the same material system. The peak aging time at the Zpl zone of 7005Al, 7005Al/15p/Al_2O_3, 7005Al/15P/SiC, and 7005Al/6p/SiC were about 16 hrs, 14 hrs, 14 hrs and 10 hrs respectively. The composites exhibit accelerated aging compared to 7005Al alloy. The effect of postweld peak aging on the horizontal hardness profile along the centerline in the heat-affected zone is shown as Fig. 6. During the postweld peak aging treatment, the hardness increased at each heat-affected zone. The maximum hardness of the Zpl zone in the 7005Al/6P/SiC particulate composites was larger, and in the 7005Al was lower. This was because the particulate concentration of 7005Al/6p/SiC particulate composites in Zpl was higher than the others, so it effectively restricted dislocation activity.

TABLE I The tensile properties of particulate metal matrix composite. (The artificial aging heated treatment)

Specimen	σ_y 0.2% (N/mm^2)	UTS (N/mm^2)	σ_f (N/mm^2)	ε_1 (%)
7005Al	290.4	350.2	346.3	14.0
7005Al/15p/SiC	258.0	322.7	302.1	12.3
7005Al/6p/SiC	260.0	324.7	306.1	11.1
7005Al/15p/Al_2O_3	312.9	390.4	379.6	14.3

3.4. The welding strength and fracture surface morphologies

The tensile properties of the 7005Al alloy and the composites after peak artificial heat treatment are shown in Table I. The tensile properties of 7005Al/6p/SiC and 7005Al/15p/SiC were quite similar. But their tensile properties were smaller than the matrix and the 7005Al/15p/Al_2O_3. Because through the artificial aging treatment, residual stress could be reduced and it could serve as a preferential nucleation site for equilibrium phase ($MgZn_2$) precipitation at the matrix–particulate interface [18]. The 7005Al/$SiC_{(p)}$ composites had a larger residual stress at the matrix–particulate interface. So the $MgZn_2$ precipitates could be easily formed at the matrix–particulate interface. A larger stress concentration and the crack initial were easily produced at the matrix–particulate interface, thus it had a poorer tensile strength than 7005Al alloy, an elongation decreased from 14.0–11.1%. For 7005Al/$Al_2O_{3(p)}$ composite, thermal strain at the matrix–particulate interface was lower than 7005Al/SiC composite. If the driving force of $MgZn_2$ precipitates formed at the interface declined, the residual stress released and stress concentration increased were similar.

The welding strengths of different joint systems are shown in Table II. For the welding strength, the workpiece went through peak aging treatment better than as welded, this was because postweld aging produced an increase in the volume fraction of fine strengthening precipitates in the Zpl zone, which led to the improvement of strength. The 7005Al joint system was greater than in the composites, because the particulate restricted the bonding of the matrix. In addition, the 7005Al/$Al_2O_{3(p)}$ joint system was larger than the 7005Al/$SiC_{(p)}$ joint system. This was because after artificial aging treatment, an increase in the stress concentration of SiC particulates caused the welding strength to decline, and the SiC particulate could be broken into a smaller size than that of Al_2O_3 particulate by shear stress as shown in Fig. 5a and c. The 6 μm SiC particulate had a higher density of particulate in the

TABLE II The welding strengths after post welding

Material system	Tensile properties			
	σ_y 0.2% (N/mm^2)	UTS (N/mm^2)	σ_f (N/mm^2)	σ_f/σ_{f^*} (%)
7005Al	217.46	223.10	217.16	65
7005Al/15p/SiC	95.72	103.31	92.75	25
7005Al/6p/SiC	71.91	77.04	71.51	19
7005Al/15p/Al_2O_3	150.43	163.69	157.29	41

σ_{f^*} is the welding strength of the work piece as welded.

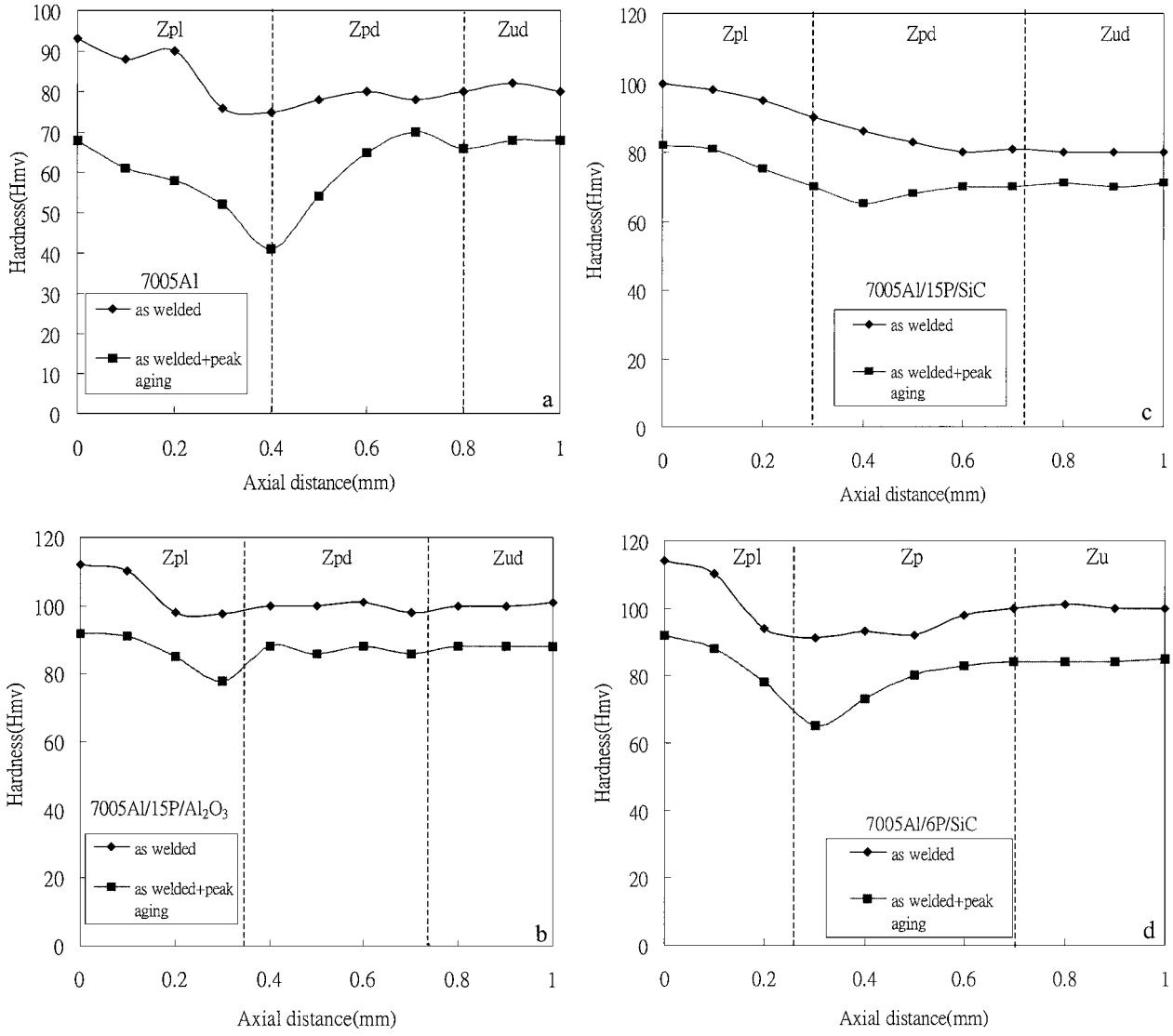

Figure 6 Effect of postweld peak aging on axial distance hardness profiles in the (a) 7005Al (b) 7005Al/15p/Al_2O_3 (c) 7005Al/15p/SiC and (d) 7005Al/6p/SiC.

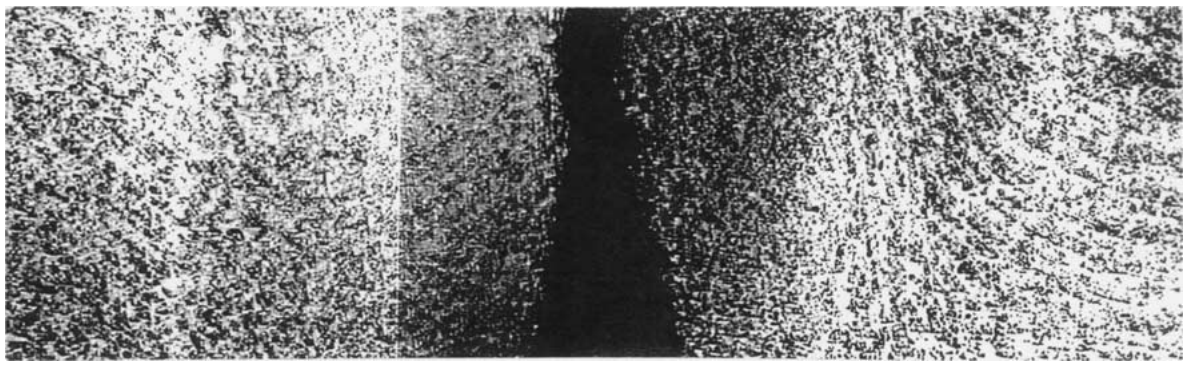

Figure 7 Micrographs of tensile fracture zone of 7005Al/15p/SiC.

Zpl zone, and stress concentration inside the Zpl zone increased by increasing the amount of SiC particulate. The 7005Al/6p/SiC had the poorest welding strength.

The tensile fracture types of different joint systems are shown in Fig. 7, All of the joint systems can be seen in the Zpl zone, because of an increase in the rate of void nucleation and an increase in the particulate density or the hardness of this zone [19].

The SEM fracture surface morphologies of 7005Al, 7005Al/$Al_2O_{3(p)}$, and 7005Al/$SiC_{(p)}$ composite workpiece after friction welding are shown in Fig. 8. In Fig. 8a, the fracture surface of 7005Al had a ductile fracture with dimples, but in Fig. 8b–d the 7005Al/particulate composites had few ductile fractures as shown. The dimension of the dimples reduced with a decrease in reinforcement particulates.

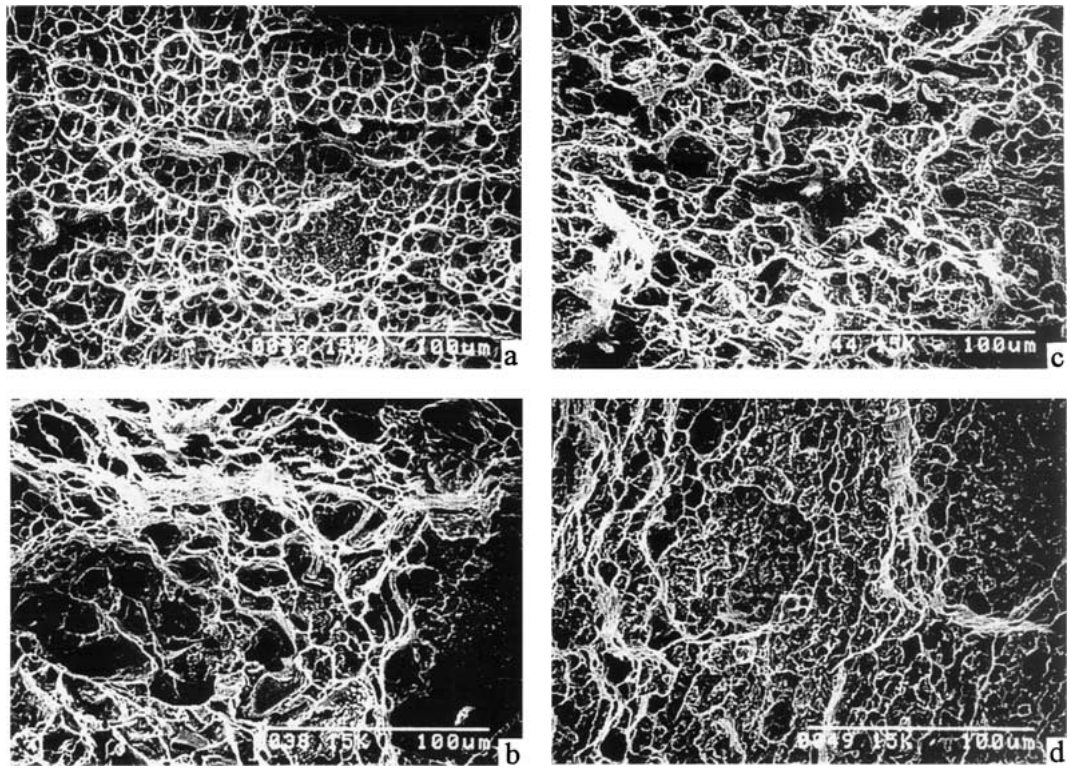

Figure 8 Micrographs of welded fractured surface (a) 7005Al (b) 7005Al/15p/Al_2O_3 (c) 7005Al/15p/SiC and (d) 7005Al/6p/SiC.

4. Conclusions

The 7005Al alloy/10 wt% 6 μm and 15 μm SiC particulate, and 7005Al alloy/10 wt% 15 μm Al_2O_3 particulate composites have been produced successfully by using a drag-push melting method, and the reinforced particulates were uniformly distributed in the matrix. The effects of peaking aging treatment on friction welding properties of the composites have been discussed, and the conclusions are as follows:

1. After friction welding, 6 μm SiC particulate could produce a larger plastic flow in the heat-affected zone. The heat-affected zone is divided into three zones: the Zpl, Zpd, and Zud zone, wherein the width of Zpl, in the 7005Al joint system is wider than the composites joint system and the 7005Al/6p/SiC composites is the smallest.
2. After posted peak aging, the peak hardness of the Zpl is the largest, and the Zud zone is the smallest, wherein the maximum hardness of the Zpl zone in the 7005Al/6p/SiC composites joint system is larger and 7005Al joint system is lower.
3. After friction welding and the posted peak aging, if SiC particulates used in the strengthening phase, and the heat-affected zone had a higher density of particulate, this would result in poorer weld strength.
4. For welded fracture surface morphology, 7005Al joint system had ductile fracture with dimples, but the composites joint system had a low-ductile fracture.

Acknowledgements

The National Science Council, Taiwan, and Republic of China supported this work.

References

1. K. K. WANG and P. NAGAPPAN, *Welding Journal Research Supplement* **49** (1970) 419.
2. K. K. WANG and WEN. LIN, *ibid.* **53** (1974) 233.
3. D. E. SPINDLER, *Welding Journal* **73** (1994) 27.
4. S. BEKIR YILBAS and Z. AHMET SAHIN, *Materials Processing Technology* **54** (1995) 76.
5. M. B. D. ELLIS, M. E. GITTOS and P. P. I. THREADGILL, *Materials World* **12** (1994) 415.
6. K. K. CHAWLA, A. H. ESMAEILI, A. K. DATYE and A. K. VASUDEVAN, *Scripta Metall. Mater* **25** (1991) 1315.
7. S. SURESH, T. CHRISTMAN and Y. SUGIMURA, *ibid.* **23** (1989) 1599.
8. J. LLORCA, A. NEEDLEMAN and S. SURESH, *Acta Metall. Mater.* **39** (1991) 2317.
9. G. J. MAHON, J. M. HOWE and A. K. VASUDEVAN, *ibid.* **38** (1990) 1503.
10. J. J. LEWANDOWSKI, C. LIU and W. HUNT, *Mater. Sci. Engin. A* **107** (1989) 241.
11. L. E. MURR, G. LIN and J. C. MC CLURE, *J. Mater. Sci.* **33** (1998) 1243.
12. M. W. MAHONEY, C. G. RHODES, J. G. FLINTOFF, R. A. SPURLING and C. C. BAMPTON, *Scripta Mater.* **36** (1997) 69.
13. J. E. HATCH, in "Aluminum Properties and Physical Metallurgy" 1st ed. (American Society for Metals, Metals Peak, Ohio, 1984) p. 185.
14. O. T. MIDLING and O. GRONG, *Acta Metal.* **42** (1994) 1611.
15. M. B. HOLLANDER, *Met. Eagng Q* **2** (1962) 14.
16. Y. B. BRECHET, J. NEWELL, S. TAO and J. D. EMBURRY, *Scripta Metallurgica et Materialia.* **28** (1993) 47.
17. C. B. LIN, C. K. MU, W. W. WU and C. H. HUNG, *Welding Journal* (1999) 100.
18. R. J. ARSENAULT and N. SHI MAT, *Material Science and Engineering* **81** (1986) 175.
19. J. K. SHANG and R. O. RITCHIE, *Acta Metallurgica.* **37** (1989) 2267.

Received 26 September 2001
and accepted 8 July 2002